Tail *et al. Journal of Inflammation* (2024) 21:34
https://doi.org/10.1186/s12950-024-00404-y

Journal of Inflammation

RESEARCH Open Access

Sonic Hedgehog reduces inflammatory response, decreases blood-spinal cord barrier permeability, and improves locomotor function recovery in an acute spinal cord injury rat model

Mohamed Tail[1,2], Hao Zhang[1], Guoli Zheng[1], Anna-Kathrin Harms[1], Maryam Hatami[3], Thomas Skutella[3], Karl Kiening[1], Andreas Unterberg[1], Klaus Zweckberger[1] and Alexander Younsi[1*]

Abstract

Background Sonic Hedgehog (Shh), extensively researched for its role in early neurogenesis and brain development, has recently been recognized for its neuroprotective potential following neuronal injuries. This study examines the immediate impact of early administered Shh on the local inflammatory response post-acute spinal cord injury in rats.

Methods Thirty-four female Wistar rats underwent either sham surgery (laminectomy; $n=10$) or clip compression/contusion spinal cord injury (SCI) at the T9 level. This was followed by implantation of an osmotic pump and a subdural catheter for continuous intrathecal delivery of Shh ($n=12$) or placebo (NaCl; $n=12$). Locomotor function was assessed at 3- and 7-days post-injury (dpi) using the Basso, Beattie, and Bresnahan (BBB) score and the Gridwalk test. Animals were euthanized after 3 or 7 days for immunohistochemical analysis of the local inflammatory reaction and immune cell migration.

Results Shh-treated rats demonstrated significant hindlimb movement and coordination improvements at 7 days post-injury, compared to controls. This enhancement was accompanied by a significant reduction in both immune cell presence and blood plasma products within spinal cord lesions, suggesting Shh's dual role in modulating immune cell migration and maintaining the integrity of the blood-spinal cord barrier. Separately, these Shh-treated rats also showed an increase in M(IL-4) polarization of macrophages, further underlining the potential therapeutic impact of Shh in post-injury recovery. Notably, these effects were not evident at three days post-injury.

Conclusion Shh application at 7 days post-injury showed immunomodulatory effects, possibly via enhanced blood-spinal cord barrier integrity, reduced immune cell migration, and increased anti-inflammatory immune cell differentiation. These mechanisms collectively contribute to enhanced locomotor recovery.

Keywords SCI, BSCB, Spinal cord injury, Sonic Hedgehog, Inflammation

*Correspondence:
Alexander Younsi
alexander.younsi@med.uni-heidelberg.de

Full list of author information is available at the end of the article

Background

Decades of spinal cord injury (SCI) research yielded a substantial understanding of the pathophysiological processes associated with this devastating injury but also of potential targets for neuroprotective or regenerative therapies. While no feasible treatment has surfaced out of these long-lasting efforts yet, recent publications still show ongoing innovation and new ideas in the fight against neurological impairment after SCI [1, 2]. As such, Sonic Hedgehog (Shh) has been identified as a potential player that could be used for SCI treatment: In preclinical studies, Shh appeared to have neuroprotective and neuroregenerative effects on the injured spinal cord and its proliferative effect on young neurons has even shown to be an adjuvant component when applied in stem-cell-based therapies [3, 4].

Inflammation and scarring, as part of the body's repair mechanisms, are needed to mitigate further trauma and separate damaged tissue from healthy tissue. However, in neurological tissue, post-injury inflammatory processes do not only exacerbate current damage rather than mitigate it, but they undermine the potential of regeneration by inducing scarring with loss of function [1, 5–7]. In the initial acute (<24 h) and subacute (24 h-7d) phases after SCI, mechanical damage sets off a cascade of post-injury inflammation processes that, in general, tend to worsen already acquired neurological deficits [5, 7]. Furthermore, patients with SCI show signs of chronic lesion site inflammation, perpetuating not only further damage but also encumbering long-term compensating mechanisms to be channeled [8, 9].

In previous works, we were able to measure long-term inflammation attenuating effects of Shh after SCI when applied one week after the injury [4]. This study aims to understand the potential impact of Shh on immediate secondary injury cascades and its role in early repair mechanisms.

Materials and methods

Animals, Treatment Characteristics, and Study Design.

We used 34 female Wistar rats (four weeks old, 160 g; *Janvier Labs*, *France*) in three treatment groups at two different timepoints (3- and 7-days post injury (dpi)): Group 1 (Shh; 3 dpi: $n=6$; 7 dpi: $n=6$), group 2 (Control; 3 dpi: $n=6$; 7 dpi: $n=6$) and group 3 (Sham; 3 dpi: $n=5$; 7 dpi: $n=5$). Rats were housed in 1815 cm^2 cages and food and water ad libitum, a 12-h light-dark cycle, and temperature at 26° were maintained. No possibility for self-training was given. Weighing of the animals was performed daily. Neurological function was assessed at baseline at 3 dpi and at 7 dpi by two independent observers. For intrathecal administration of Shh or placebo we used osmotic micropumps (*Alzet*, *USA*) implanted immediately after SCI. Two animals in group 1 died during the experiment, resulting in a total sample size of $n=32$ rats. The study was terminated with the perfusion of all animals at respective time points (3 dpi, 7 dpi). All experimental protocols were approved by the Animal Care Committee of the federal government.

Surgical interventions

We described the performed surgical interventions in our previous work [10]. In short, animals were put under general anesthesia with isoflurane (1.5–3%) and a 1:1 mixture of O_2 and N_2O. Laminectomy was performed at the T9 level. After exposing the spinal cord, we reproduced a contusion–compression injury using a 28 g modified aneurysm clip (*Fehlings Laboratory*, *Canada*). We applied it around the spinal cord, shut and sustained it for 60 s. To administer Shh or placebo to the spinal cord, we implanted a subcutaneous osmotic pump (*model 1007D; Alzet*, *USA*) right after SCI and placed the tip of the connected rat microcatheter subdurally via a skip laminectomy of T11 and fixation to the paraspinal muscles. Osmotic pumps were preloaded with 100 µl of Shh (50 ng/ml; *R&D Systems*, *USA*; group 1) or 0.9% NaCl (group 2; Control), primed in a 2-hour loading cycle in 0.9% NaCl at room temperature and randomly assigned to the animals intraoperatively. After implantation, the osmotic pumps delivered the loaded substances directly to the epicenter of the lesion for up to seven days or until the time of sacrifice. Sham animals (group 3) received a laminectomy of T9 and T11 only. The postoperative protocol included antibiotic prophylaxis using 4 mg/kg moxifloxacin p.o. (*Fresenius*, *Germany*) analgesia using 0.05 mg/kg buprenorphine s.c. (*Bayer*, *Germany*) and 2 mg/kg meloxicam s.c. (*Boehringer-Ingelheim*, *Germany*), as well as fluid substitution (3–5 ml 0.9% NaCl s.c.) for up to 5 days. Bladders were manually voided twice daily until reflexive bladder function had recovered.

Assessment of locomotor function

To objectively assess hindlimb movement we performed an open-field test and evaluated it according to the Basso-Beattie-Bresnahan locomotor rating scale (BBB) at 1, 3 and 7 dpi. Points were given for hindlimb movement, weight support, coordination, joint involvement, tail movement, and trunk position in a four-minute run, evaluated by two blinded observers (Table 1). Results were averaged and statistically analyzed (0–21 points) [11].

Furthermore, the Gridwalk test was performed on a 1 m long runway of evenly spaced metal bars with bars randomly missing. Stepping errors were counted by two blinded observers for every misplaced step per hindlimb and averaged over three trials. Baseline training and evaluation were performed one day prior to injury, at 3 dpi and 7 dpi [12].

Table 1 To evaluate post-SCI locomotor function, the Basso, Beattie, Bresnahan (BBB) score for rodents was used [11]. Animals were tested at 1, 3 and 7 dpi. Two blinded observers scored each rat in an open field box

Score	Description
0	No observable hindlimb (HL) movement
1	Slight movement of one or two joints, usually the hip and/or knee
2	Extensive movement of one joint or extensive movement of one joint and slight movement of one other joint
3	Extensive movement of two joints
4	Slight movement of all three joints of the HL
5	Slight movement of two joints and extensive movement of the third
6	Extensive movement of two joints and slight movement of the third
7	Extensive movement of all three joints of the HL
8	Sweeping with no weight support or plantar placement of the paw with no weight support
9	Plantar placement of the paw with weight support in stance only (i.e., when stationary) or occasional, frequent, or consistent weight supported dorsal stepping and no plantar stepping
10	Occasional weight supported plantar steps, no forelimb (FL)-HL coordination
11	Frequent to consistent weight supported plantar steps and no FL-HL coordination
12	Frequent to consistent weight supported plantar steps and occasional FL-HL coordination
13	Frequent to consistent weight supported plantar steps and frequent FL-HL coordination
14	Consistent weight supported plantar steps, consistent FL-HL coordination; and predominant paw position during locomotion is rotated (internally or externally) when it makes initial contact with the surface as well as just before it is lifted off at the end of stance or frequent plantar stepping, consistent FL-HL coordination, and occasional dorsal stepping
15	Consistent plantar stepping and consistent FL-HL coordination; and no toe clearance or occasional toe clearance during forward limb advancement; predominant paw position is parallel to the body at initial contact
16	Consistent plantar stepping and consistent FL-HL coordination during gait; and toe clearance occurs frequently during forward limb advancement; predominant paw position is parallel at initial contact and rotated at lift off
17	Consistent plantar stepping and consistent FL-HL coordination during gait; and toe clearance occurs frequently during forward limb advancement; predominant paw position is parallel at initial contact and lift off
18	Consistent plantar stepping and consistent FL-HL coordination during gait; and toe clearance occurs consistently during forward limb advancement; predominant paw position is parallel at initial contact and rotated at lift off
19	Consistent plantar stepping and consistent FL-HL coordination during gait; and toe clearance occurs consistently during forward limb advancement; predominant paw position is parallel at initial contact and lift off; and tail is down part or all of the time
20	Consistent plantar stepping and consistent coordinated gait; consistent toe clearance; predominant paw position is parallel at initial contact and lift off; tail consistently up; and trunk instability
21	Consistent plantar stepping and coordinated gait, consistent toe clearance, predominant paw position is parallel throughout stance, consistent trunk stability, tail consistently up

Immunofluorescence staining and imaging analysis

After animal sacrifice and perfusion with cold phosphate buffered saline (PBS) and 4% paraformaldehyde (PFA), as previously described [4, 13] we obtained spinal cord pieces +/- 10 mm from the epicenter which were incubated with 4% PFA for 24 h and 30% sucrose for 48 h. The spinal cord pieces were then embedded with Tissue-TEK® (*Sakura Finetek Europa B.V.*, *Netherlands*) on dry-ice and cut into consecutive 30 µm thick cross-sections using a cryostat (*Leica Biosystems*, *Germany*). Finally, spinal cord cross-sections were placed on specimen slides, dried, and stored at -80 °C until further usage.

For immunofluorescence staining, slides were thawed at room temperature and washed three times with PBS. The cross-sections were then subjected to the following immunofluorescence staining protocol: PBS was removed, and a blocking solution containing 0.3% Triton-X100, 5% milk powder, and 1% bovine serum albumin (all *Sigma-Aldrich*, *USA*) was added for one hour at room temperature. Then, the cross-sections were incubated with primary antibodies diluted in the blocking solution at 4° C overnight.

The following primary antibodies were used: Anti-β-catenin (1:200; rabbit; *Abcam*, *USA*) for the evaluation of adherens junction complexes, anti-Fibrinogen (1:500; mouse; *Santa Cruz*, *Germany*) for blood plasma protein leakage, anti-TMEM119 (1:200; rabbit; *Abcam*, *USA*) as a marker for resident microglia, anti-Iba1 (1:200; goat; *Novus Biologicals*, USA) for macrophages and microglia, anti-CD206 (1:200; goat; *Bio-Rad*, *Germany*) and anti-iNOS (1:100; mouse; *Abcam*, *USA*) for the identification of M(IFN-γ)- and M(IL-4)- macrophages.

Next, we washed the cross-sections three times with PBS and subjected them to incubation with the secondary antibodies diluted in a blocking solution without Triton-X100 for one hour at room temperature. The following secondary antibodies were used: Alexa Fluor 557 donkey anti-mouse (1:400; *R&D Systems*, *USA*), Alexa Fluor 647 donkey anti-rabbit (*1:400; Abcam*, *USA*), and Alexa Fluor 405 donkey anti-goat (1:400; *Abcam*, *USA*).

Using a confocal laser scanning microscope (*LSM 700; Carl-Zeiss, Germany*) we obtained images of each cross-section at 10x magnification in an 8-bit-format with tile scan function (speed of 4, gain of 800). Four wavelength channels (Alexa Fluor-405 nm, GFP-488 nm, Alexa Fluor 568 nm, Alexa Fluor 647 nm) were used.

To quantitatively evaluate the different cell types on the cross-sections, we applied a semi-automatic counting-algorithm for ImageJ2 (National Institute of Health, Bethesda, USA), as previously described [4]. In short, images were split into single channels using the ImageJ2 software [14]. Then, a region of interest (ROI) was placed, covering the whole cross-sectioned spinal cord. Following transformation into a binary image using the "IsoData-threshold" function, a binary image was formed and the "Analyze" function was used to determine the cell count. To quantify co-labeled cells within the selected ROI, we used the "Image calculator" function to combine channels before transformation into binary images. To avoid the inclusion of artifacts, only cells with an area of 50-2000 μm^2 were considered. Cell counts where then divided by the area of the ROI (derived with the "Measure" function), and the results of 40 cross-sections per animal (+/- 600 µm from the lesion epicenter) were averaged and expressed as cells/mm^2.

To quantitatively evaluate BSCB leakage (ß-Catenin and Fibrinogen), the immunointensity of the respective antibody fluorescence was quantified, as previously described [4, 15]. Briefly, we split images into single channels with the ImageJ2 software, set ROIs covering the whole cross-sectioned spinal cord, and used the "Measure" function to derive the area and the integrated density in pixels (pi). Integrated density values were then divided by the area of the ROI, the results of 40 cross-sections per animal (+/- 600 µm from the lesion epicenter) were averaged and expressed as pi/mm^2.

Statistical analysis

We performed Shapiro-Wilk normality tests prior to normality assumption before all parametric analyses. One-way analysis of variance (ANOVA) followed by post hoc Tukey-HSD tests were used for the statistical comparison of means between multiple groups. Two-way ANOVA followed by post hoc Tukey-HSD tests were performed for the statistical comparison of means between multiple groups among multiple time points. For the comparison of two groups, unpaired student t-tests were performed. All results are given as mean ± standard error of the mean (SEM), and $p<0.05$ was considered significant. All statistical analyses were done with the software Prism (*GraphPad Software, USA*) in version 9.

Results

Shh-treatment might decrease BSCB permeability

Fibrinogen is a blood serum protein that, under physiological circumstances, cannot pass the BSCB. To understand Shh-mediated effects on BSCB permeability, we examined the intramedullary concentration of Fibrinogen after SCI as a surrogate marker for perivascular leakage. While there was no significant difference between the untreated and Shh-treated animals at 3 dpi (12.51 ± 0.9468 pi/mm^2 vs. 16.09 ± 1.846 pi/mm^2; $p=0.1721$), we observed significantly less intramedullary Fibrinogen at 7 dpi with the Shh-treatment (16.16 ± 1.208 pi/mm^2 vs. 26.03 ± 1.192 pi/mm^2; $p<0.01$). These results might indicate a Shh-related decrease of the post-traumatic BSCB permeability.

The highly regulated permeability of the BSCB is largely dependent on cellular adhesion complexes. An Shh-associated increase of tight junction proteins has been well documented. Next to the Shh-pathway, the Wnt/β-Catenin pathway has been deemed important for maintenance and repair of BBB [16–18].

We chose to examine the expression of β-Catenin, an adherens junction and crucial Wnt/β-Catenin-pathway protein, to assess possible Shh-mediated alterations.

Interestingly, Shh treated animals showed significantly higher β-Catenin levels compared to untreated animals at 3 dpi (11.06 ± 0.749 pi/mm^2 vs. 3.869 ± 0.910 pi/mm^2; $p=0.0213$) as well as at 7 dpi (38.59 ± 3.386 pi/mm^2 vs. 29.36 ± 2.015 pi/mm^2; $p=0.0234$) (Fig. 1).

These results may implicate a Shh-mediated modulation of β-Catenin concentration and consecutively interaction with the Wnt/β-Catenin pathway.

Shh-pathway activation might reduce trans-BSCB migration of blood-borne immune cells

Recent publications attribute an anti-inflammatory effect to the Shh-pathway activation in neuronal settings [19–22]. The underlying mechanisms of these effects are not fully understood. However, the extent of neuro-inflammation is associated with the amount of pro-inflammatory proteins and cells present which in turn might be related to trans-BSCB migration [23, 24]. We thus semiautomatically quantified macrophages in the spinal cord expressing Iba-1 in the absence of TMEM119, indicating a blood-borne origin and potential trans-BSCB migration.

At 7 dpi, the presence of such Iba-1^+/TMEM119^- cells in the injured spinal cord was significantly lower in Shh-treated animals than in untreated animals (838.54 ± 43.57 cells/mm^2 vs. 1093.54 ± 48.87 cells/mm^2; $p=0.0027$), which might be attributed to Shh-related tightening of the BSCB. This effect could not be seen at 3 dpi, where Shh-treated and Control animals did not significantly differ in the number of infiltrated cells (1091.45 ± 96.46 cells/

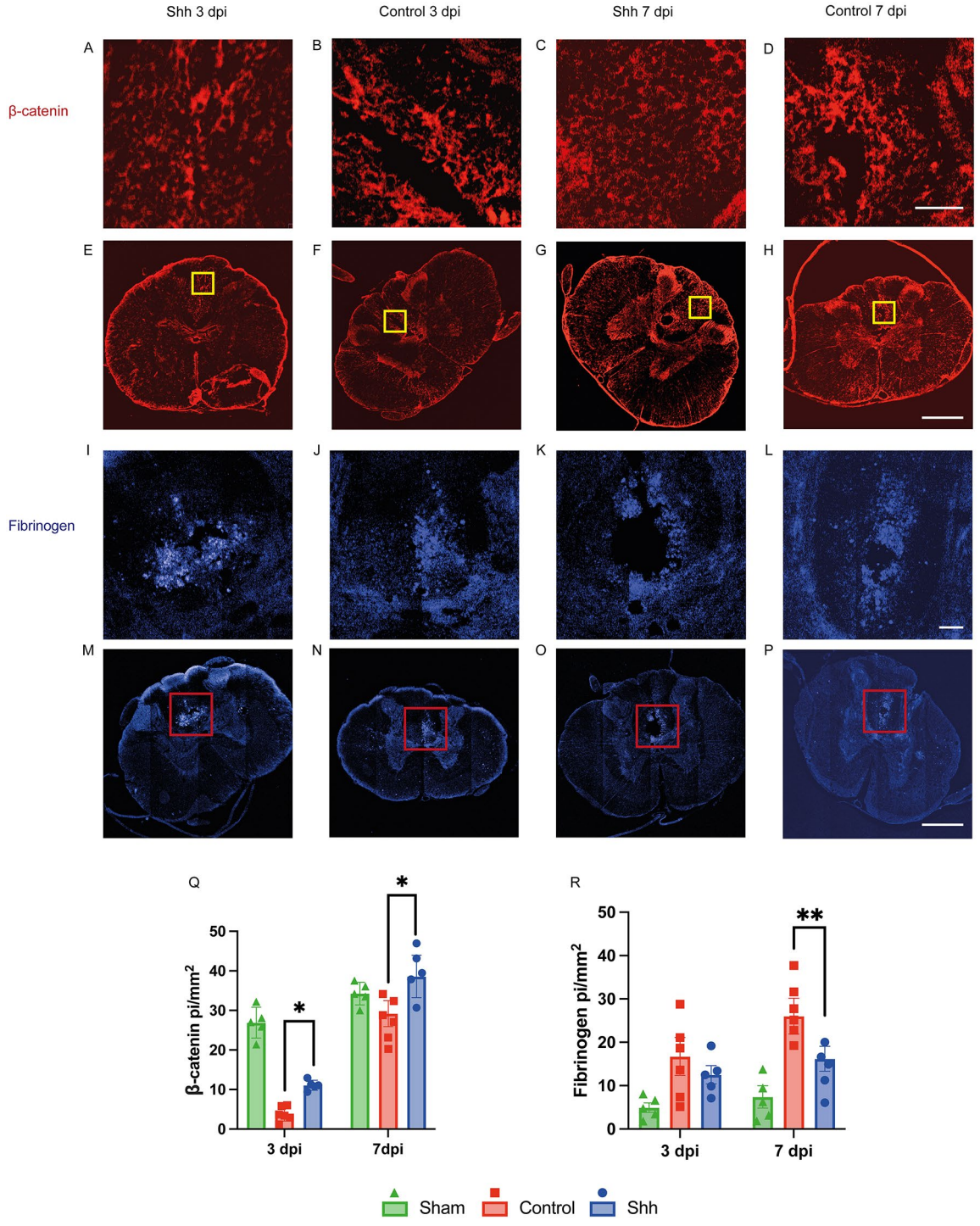

Fig. 1 (**A-P**) Cross-sectional images of lesioned spinal cords in the Shh- and Control group 3- and 7-days post injury (dpi), stained for β-catenin (red) and Fibrinogen (blue) at different magnifications: 20x (**A-D**; scale bar: 150 µm), 10x (I-L; scale bar: 75 µm), and 10 × (4x4 tile-scans, E-H + M-P; scale bar: 500 µm). (**Q**) β-catenin staining (red) shows a significantly higher concentration in Shh-treated animals ($n = 5$) compared to untreated animals at 7 dpi ($p = 0.0234$, $n = 6$), as well as at 3 dpi ($p = 0.0213$). Blue staining highlights intramedullary evidence of Fibrinogen extravasation (I-P; blue). (**R**) While there was no significant difference in Fibrinogen accumulation between Shh-treated ($n = 5$) and untreated animals ($n = 6$) at 3 dpi, at 7 dpi, less Fibrinogen extravasation was observed in the Shh group ($n = 5$) compared to the Control group ($p < 0.01$, $n = 6$). Data are expressed as mean ± SEM pi/mm^2. Statistical analysis was conducted using one-way ANOVA with post hoc Tukey-HSD tests (*$p < 0.05$, **$p < 0.01$)

mm^2 vs. 1043.38±61.40 cells/mm^2; $p=0.837$). Furthermore, at 7 dpi, Shh-treated animals also displayed less intramedullary TMEM119$^+$ cells compared to untreated animals in the Control group (954.13±60.14 cells/mm^2 vs. 1262.78±60.66 cells/mm^2; $p<0.0001$), while at 3 dpi no significant difference was found (417.84±68.27 cells/mm^2 vs. 483.30±45.50 cells/mm^2; $p=0.829$). Since the expression of TMEM119 characterizes resident microglia, this finding might be interpreted as a reduced immune cell activation under the Shh pathway activation (Fig. 2).

Shh is related to anti-inflammatory polarization of macrophages

The post-injury secondary inflammatory changes in the spinal cord are partly defined by the prevalent ratio of immune cells in situ [25]. A transition from pro-inflammatory to anti-inflammatory macrophages is thereby associated with less neuronal damage and improved locomotor function rehabilitation after SCI [25–27]. To determine the polarization of macrophages in the injured spinal cord, we used the markers iNOS for the M(IFN-γ)- and CD206 for the M(IL-4)-phenotype and semiautomatically counted cells with either only iNOS- or CD206-expression, thereby disregarding macrophages still in transition (expressing both, iNOS and CD206).

At 3 dpi we could not find a difference between Shh-treated and Control animals in neither the number of iNOS$^+$/CD206$^-$ M(IFN-γ)-polarized macrophages (M(IFN-γ)) (71.97±12.45 cells/mm^2 vs. 93.01±15.33 cells/mm^2; $p=0.168$), nor iNOS$^-$/CD206$^+$ M(IL-4)-polarized macrophages (M(IL-4)) (94.32±20.32 cells/mm^2 vs. 98.71±11.49 cells/mm^2; $p=0,973$) in situ. However, the Shh-treatment led to a significantly lower number of M(IFN-γ) compared to the Control group 7 dpi (32.85±2.54 cells/mm^2 vs. 72.66±6.99 cells/mm^2; $p<0.001$). Furthermore, Shh-treated animals showed a higher count of M(IL-4) than the untreated Control animals (150.78±24.93 cells/mm^2 vs. 70.65±10.37 cells/mm^2; p=$p<0.001$), indicating that Shh might be related to an increased transition from the pro-inflammatory M(IFN-γ)- to the anti-inflammatory M(IL-4)-phenotype (Fig. 3).

Shh-application is associated with improved functional recovery of hindlimb locomotion

In order to examine acute effects off Shh on the functional outcome after SCI we tested for hindlimb locomotion using the Gridwalk test and the BBB locomotor rating scale. The Gridwalk test did not display significant differences between the Shh- and the Control-group at 3 dpi (23.07±2.64 stepping errors vs. 25.89±2.61 stepping errors; $p=0.613$) and 7 dpi (18.10±2.75 vs. 20.67±2.63 stepping errors; $p=0.643$). The evaluation of the BBB scores at 3 dpi showed no significant difference between both group (Shh 2.47±0.42 points vs. Control 1.69±0.170 points; $p=0.183$). However, at 7 dpi, a significant and relevant improvement of hindlimb locomotor function in Shh-treated animals compared to untreated Control animals could be observed (7.857±1.262 points vs. 3.583±1.175 points; $p<0.001$, Fig. 4).

Discussion

SCI is a devastating diagnosis for patients and involved relatives. Years of neuroregenerative research advanced our understanding of pathophysiological processes but failed to find a feasible treatment to rehabilitate patients. Promising substances and treatments have previously been advanced into phase II/III trials [1]; however, none of these have yielded relevant results yet [28, 29].

It is imperative to understand that treatment begins with prevention. For example, improved vehicle and work safety measures have shown a steady decrease in traumatic SCI in Europe and the US. After initial injury, further therapeutic options are scarce. We believe that breaking the cycle of secondary injury after SCI as prevention of further damage might be a treatment option itself, leading to improved functional outcomes and life quality.

Shh and the Shh-pathway have been extensively researched on their morphogenic as well as proto-oncological capability [30–32]. Recent publications introduced the neuroprotective and anti-inflammatory features of Shh on neuronal tissue. Furthermore, its endogenous activation after neuronal injury [3, 21], as well as its effect on the recruitment and guidance of undifferentiated neuronal cells has been associated with the active repair of neuronal damage [33].

Therefore, through our experimental study design, we aimed to understand Shh-pathway-associated repair and defensive mechanisms in the acute and early subacute SCI environment. Previous studies examining intrathecal substance-application had varying timepoints of insertion ranging from 3 days pre-injury to 7 days post-injury [34–36]. Since our aim was to study and understand Shh-mediated changes in the acute and subacute phase, our approach to implant the intrathecal pump at the same time as SCI seemed a sensible approach. Like other researchers, we suspect that crucial effects of treatment might take place early, since the BSCB is most vulnerable in the acute stages of injury [37, 38].

Interestingly, we were able to show that Shh-treated rats exhibit significantly less plasma protein leakage after injury compared to untreated animals. This is in accordance with prior findings. For example, Alvarez et al. 2011 described increased Fibrinogen extravasation in Cyclopamine injected mice, a potent Shh-pathway inhibitor [39]. The underlying mechanisms are still unknown.

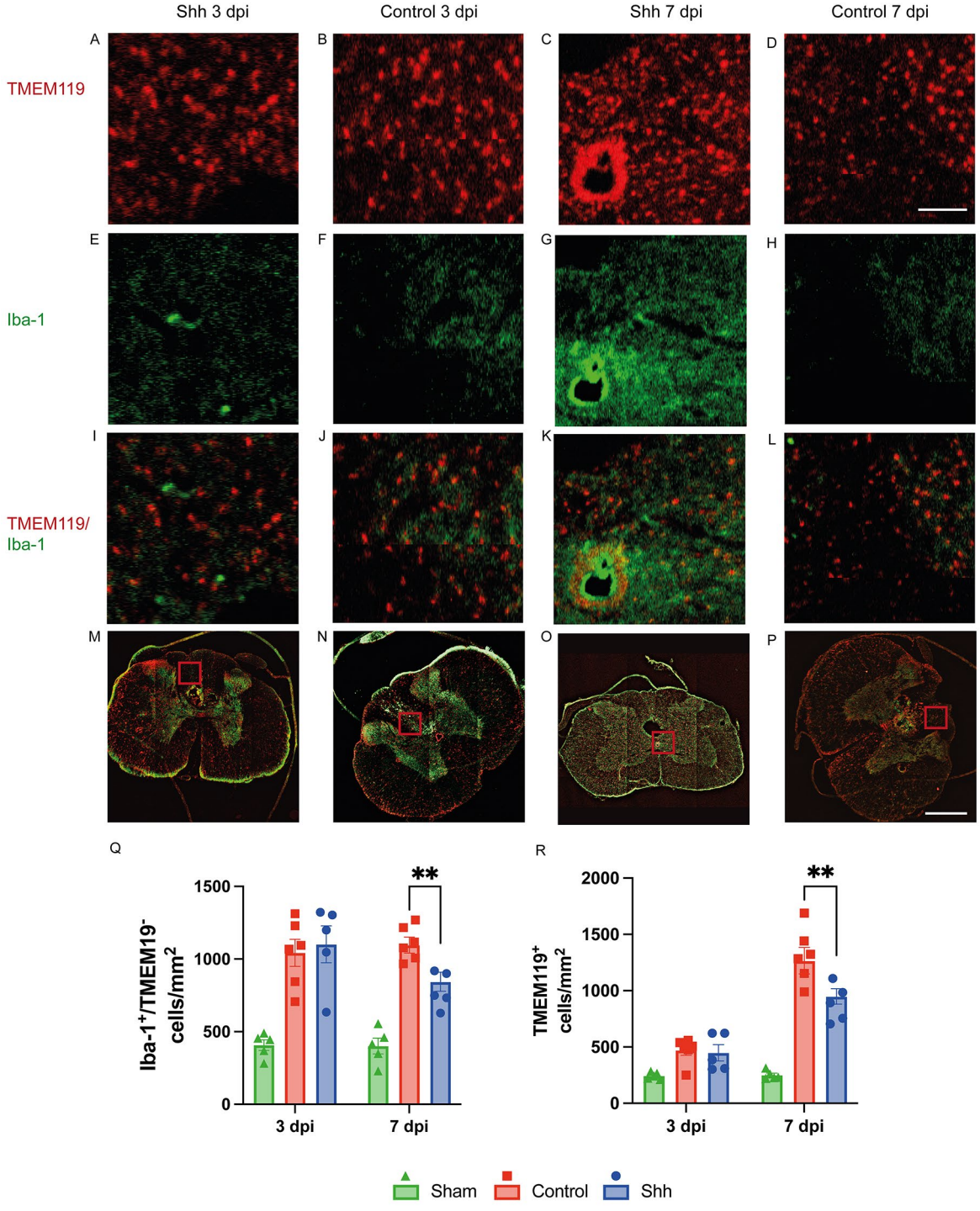

Fig. 2 (**A-L**) 20x-magnification cross-sectional images of lesioned spinal cords in the Shh- and Control group 3- and 7-days post injury (dpi) stained for TMEM119 (red; **A-D**) and Iba-1 (green; **E-H**), along with composite images (**I-L**; scale bar: 150 µm). (M-P) The corresponding 10x-magnification 4×4 tile-scans are presented as composite images, with the overlying inlets (**A-L**) depicted in red (scale bar: 500 µm). (**Q**) TMEM119 is expressed by intramedullary resident microglia, while blood-borne immune cells lack TMEM119 expression. Therefore, subtracting TMEM119$^+$ cells from the total Iba-1$^+$ macrophage population enables the identification of infiltrating macrophages. Shh-treated animals ($n=5$) exhibited a significantly lower number of Iba-1$^+$/TMEM119$^-$ infiltrating immune cells compared to untreated controls ($n=6$) at 7 dpi ($p=0.0027$). (**R**) Additionally, fewer TMEM119$^+$ resident microglia were observed in the Shh group ($n=5$) compared to the Control group ($n=6$) at 7 dpi ($p<0.01$). Data are presented as mean ± SEM cells/mm^2. Statistical analysis was performed using one-way ANOVA with post hoc Tukey-HSD tests (**$p<0.01$)

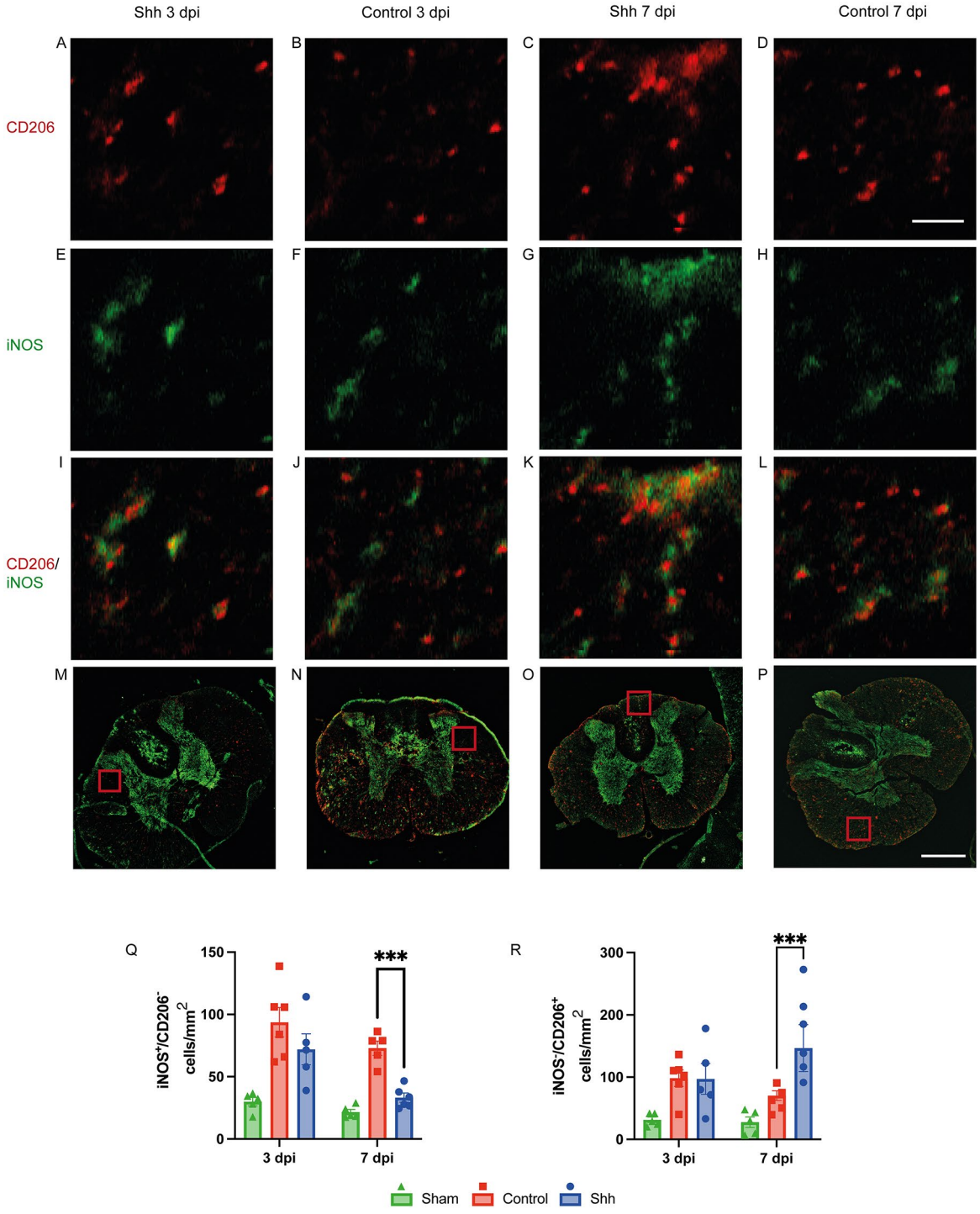

Fig. 3 (**A-L**) 20x-magnification cross-sectional images of lesioned spinal cords in the Shh- and Control group 3- and 7-days post injury (dpi) stained for CD206 (red; A-D), iNOS (green; E-H), and composite images (I-L; scale bar: 150 µm). (M-P) The corresponding 10x-magnification 4 × 4 tile-scans are presented as composite images, with the overlying inlets (**A-L**) depicted in red (scale bar: 500 µm). Due to the fluid nature of M(IFN-γ) to M(IL-4) polarization, distinguishing between the expression of CD206 and iNOS remains challenging. Therefore, iNOS-expressing cells without CD206 co-staining ($iNOS^+/CD206^-$) were counted as indicative of M(IFN-γ)-polarized macrophages, while $iNOS^-/CD206^+$ cells were considered indicative of M(IL-4)-polarized macrophages. (Q) While no significant difference was observed at 3 dpi, Shh treatment ($n = 5$) was associated with significantly fewer M(IFN-γ)-polarized, pro-inflammatory macrophages compared to untreated controls at 7 dpi ($p < 0.001$, $n = 6$). (R) Simultaneously, an increase in M(IL-4)-polarization towards an anti-inflammatory macrophage phenotype was noted under Shh treatment ($n = 5$) compared to untreated animals ($p < 0.001$, $n = 6$). Data are expressed as mean ± SEM cells/mm^2. Statistical analysis was performed using one-way ANOVA with post hoc Tukey-HSD tests (***$p < 0.001$)

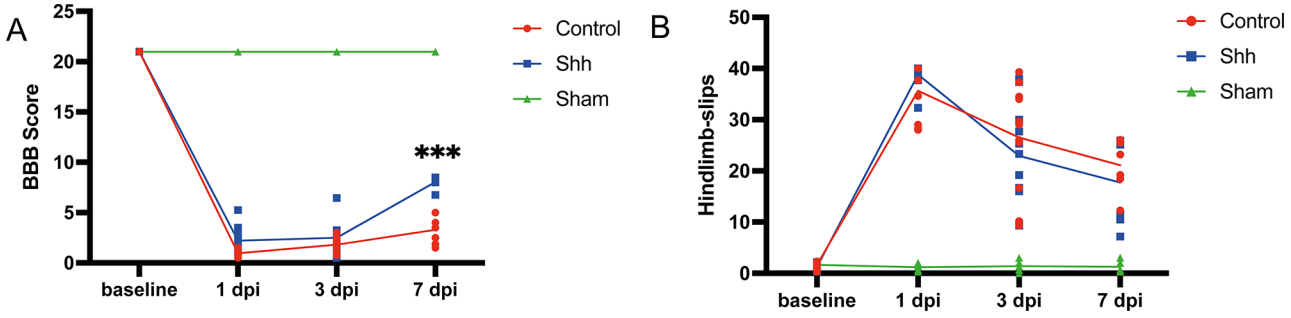

Fig. 4 (**A**) Shh-treated animals ($n=5$) demonstrated improved locomotor function, as indicated by significantly higher BBB scores at 7 days post-injury (dpi) compared to untreated control animals ($p<0.001$, $n=6$). (**B**) In the Gridwalk test, both the Shh- and the control group showed a similar rate of stepping errors at 3 dpi and 7 dpi (for both timepoints: Shh: $n=5$, Control: $n=6$). Experiments were conducted in triplicate, with data interpreted by two blinded observers and averaged. Data are expressed as BBB points or stepping errors and presented as mean ± SEM. Statistical analysis was performed using two-way ANOVA with post hoc Tukey-HSD tests (***$p<0.001$)

Different effector proteins have been identified as being induced by GLI-1, one of the main transcriptors activated by the Shh-pathway, e.g., Netrin-1 and β-catenin [40, 41].

In our study, we could depict a significant increase in β-catenin concentration in Shh-treated animals. The dual function of β-catenin not only serves as a signal transducer - essential to the Wnt/β-catenin pathway - but also as a vital adherents junction protein to the blood-brain-barrier complex [42]. In review of known data, the effects of the Wnt/β-catenin-pathway go beyond tight junction modulation to increase the BBB. Induction of BBB properties in endothelial cells, regulation of transcytosis as well as reduction of inflammatory responses are processes by which the pathway might enhance the BBB. Like Shh-pathway activation, Wnt-/β-catenin pathway activation is associated with increased expression of tight junction proteins such as ZO-1, Occlodin and Claudin 5. [43–45]. Changes in the perivascular concentration of β-catenin are associated with changes in BSCB permeability, and as such they are commonly used as an indicator for BBB and BSCB disruption [46]. The Shh-related increase in β-catenin might suggest a synergistic effort on BSCB tightening attenuation. [47]

The disruption of the BSCB in trauma is considered part of the posttraumatic inflammation process, as it facilitates an influx of immune cells and other blood-derived immune factors to further the immune response on site [42, 48, 49]. This might be the key reason for our observed decreased migration of recruited macrophages into the lesion site. In previous experiments we were able to show attenuated neuroinflammation via Shh-pathway activation in vitro and in vivo [4, 15]. One key mechanism might be the described BSCB tightening that disallows immune cell migration. Albeit the association between BSCB and immune cell immigration might seem self-evident, it has not been thoroughly elaborated yet and will require further investigation.

While pro-inflammatory M(IFN-γ)-macrophages are associated with IL-12, IL-23, and tumor necrosis factor-α (TNF-α) expression and help "irrigate" the lesion site, M(IL-4)-macrophages are characterized inter alia by CD206 surface proteins and show secretion of anti-inflammatory interleukins and chemokines (IL-10, CCL17, CCL18, and CCL22) to counter the inflammatory response and start the wound healing phase [50–53]. Extensive research on M(IFN-γ)/M(IL-4) macrophage polarization highlights different activation mechanisms, e.g., time after injury. In short, in the classical macrophage polarization paradigm, naïve macrophages are pushed into the M(IFN-γ) phenotype if exposed to lipopolysaccharide (LPS) or TNF- α, while the M(IL-4) phenotype polarization is dependent on anti-inflammatory cytokines, e.g. IL-4, IL-10, IL-13 [53]. , which occurs delayed to injury. In an extensive review by Hillenbrand et al., analysis of local cytokine levels in post-SCI animal rodents showed an early (within hours) upregulation of proinflammatory cytokines IL-1β, TNFα, IL-6, and late upregulation of immunomodulatory cytokines IL-4, IL-10, IL-13 starting earliest at 24 h to 7 dpi [54].

In our experiment, we observed an Shh-associated increase in M(IL-4) polarized macrophages, characterized by CD206-expression and a decrease in M(IFN-γ) polarized macrophages, indicative through iNOS-expression. Although in vivo markers of M(IFN-γ)/M(IL-4) phenotypes are fluid and the separation effect is often difficult to determine, iNOS (M(IFN-γ)) and CD206 (M(IL-4)) are consistent, valid, widespread, and commonly recognized to differentiate M(IFN-γ) and M(IL-4) phenotypes [51, 55–57]. The observed increase of M(IL-4) polarized macrophages is typically considered anti-inflammatory and has been associated with the transition into the regenerative wound healing phase by other authors [50, 52, 53].

Our findings on the effects of intrathecally applied Shh on the integrity of the BSCB and the damping of the inflammatory response after SCI might explain the mild improvement of hindlimb locomotion observed 7 dpi. In our assessment of locomotor function, we used the

grid-walk test which did not display differences between Shh and Control animals at 3 and 7 dpi, and the BBB open field score which showed significant and relevant improvements of Shh-treated animals at 7 dpi.

The BBB scoring system, appears to offer adequate sensitivity for early-stage evaluations, effectively distinguishing minor variations in the movement of hindlimbs [58, 59]. Although assessing locomotor function in our study had its challenges, our results align with prior experiments: Activation of the Shh-pathway has been previously linked to a reduction in inflammatory responses, and some studies have also directly correlated this pathway's activation with improvements in locomotor function [10, 60, 61]. Similarly, other SCI research that focused on reducing inflammation also reported enhanced locomotor abilities in rodents [62, 63]. For instance, research by Li et al. demonstrated that mice lacking the TREM1 gene, which encodes an immune receptor that promotes inflammation, exhibited improved locomotion due to reduced inflammation [62]. These findings lend further support to the idea that managing neuroinflammation early on might be key to successful long-term recovery of locomotor function post-SCI.

Finally, several limitations need to be considered. The Gridwalk test is a recognized method for assessing coordination and weight-bearing ability following experimental SCI. However, it's important to highlight that this test is typically conducted during later recovery phases post-injury [64]. Therefore, the subpar performance observed in the early phase evaluations of locomotor function using the Gridwalk test should have been expected. Upon reflection, we hypothesize that in the initial stages of SCI assessment, up to 7 dpi, rodents may not yet have regained sufficient coordination and muscular strength to reliably and meaningfully complete complex neurological tests with our injury model. Furthermore, we were unable to incorporate lesion size and perifocal edema volume in this study due to capacity limitations. We acknowledge that including such assessments would have enhanced our understanding of the potential effects of Shh-treatment.

Conclusion

Topical administration of exogenous Shh to the injured spinal cord may help mitigate neuroinflammation. However, the specific effector processes remain unclear. Activation of the Shh pathway may reinforce the BSCB and potentially correlate with macrophage polarization from a pro-inflammatory M(IFN-γ) state to a regenerative M(IL-4) state during the subacute phase of SCI, which could enhance locomotor function recovery. Further research is needed to comprehensively ascertain the immediate impacts of Shh on neuroinflammation.

Acknowledgements
We would like to thank our colleagues of the Department of Neuroanatomy as well as our colleagues at the INBC Heidelberg (Dr. Claudia Pitzer) for their generous help and advice.

Author contributions
Conceptualization, Younsi, A. and Zweckberger, K.; methodology, Hatami, M., Skutella, T. and Younsi, A.; validation, Younsi, A. and Tail, M.; formal analysis, Tail, M. and Younsi, A.; investigation, Tail. M, Zheng, G., Younsi, A.; resources, Skutella, T., Hatami, M., Younsi, A. and Zweckberger, K.; data curation, Tail, M., Zheng, G., Zhang, H., Harms, A. and Hatami, M.; writing—original draft preparation, Tail, M.; writing—review and editing, Younsi, A and Zheng, G.; supervision, Younsi, A., Zweckberger, K. and Unterberg, A.; project administration, Younsi, A.; funding acquisition, Younsi, A., Zweckberger, K. and Unterberg. All authors have read and agreed to the published version of the manuscript.

Funding
Open Access funding enabled and organized by Projekt DEAL.

Data availability
No datasets were generated or analysed during the current study.

Declarations

Ethical approval
All experimental protocols were approved by the Animal Care Committee of the federal government of Baden-Württemberg, Germany.

Conflict of interest
The authors declare that the research was conducted in the absence of any commercial or financial relationships that could be construed as a potential conflict of interest.

Competing interests
The authors declare no competing interests.

Author details
[1]Department of Neurosurgery, Heidelberg University Hospital, 69120 Heidelberg, Germany
[2]Department of Neurology, Heidelberg University Hospital, 69120 Heidelberg, Germany
[3]Department of Neuroanatomy, Institute for Anatomy and Cell Biology, Heidelberg University, 69120 Heidelberg, Germany

Received: 6 February 2024 / Accepted: 20 August 2024
Published online: 03 September 2024

References

1. Venkatesh K, Ghosh SK, Mullick M, Manivasagam G, Sen D. Spinal cord injury: pathophysiology, treatment strategies, associated challenges, and future implications. Cell Tissue Res. 2019;377(2):125–51.
2. Shao A, Tu S, Lu J, Zhang J. Crosstalk between stem cell and spinal cord injury: pathophysiology and treatment strategies. Stem Cell Res Ther. 2019;10(1):238.
3. Bambakidis NC, Wang RZ, Franic L, Miller RH. Sonic hedgehog-induced neural precursor proliferation after adult rodent spinal cord injury. J Neurosurg. 2003;99(1 Suppl):70–5.
4. Zhang H, Younsi A, Zheng G, Tail M, Harms AK, Roth J et al. Sonic hedgehog modulates the inflammatory response and improves functional recovery after spinal cord injury in a thoracic contusion-compression model. Eur Spine J. 2021.
5. Ahuja CS, Nori S, Tetreault L, Wilson J, Kwon B, Harrop J, et al. Trauma Spinal Cord Injury—Repair Regeneration Neurosurg. 2017;80(3S):S9–22.
6. Anjum A, Yazid MDI, Fauzi Daud M, Idris J, Ng AMH, Selvi Naicker A, et al. Spinal cord Injury: pathophysiology, Multimolecular interactions, and underlying recovery mechanisms. Int J Mol Sci. 2020;21(20):7533.
7. Orr MB, Gensel JC. Spinal cord Injury scarring and inflammation: therapies targeting glial and inflammatory responses. Neurotherapeutics. 2018;15(3):541–53.

8. Li X, Li M, Tian L, Chen J, Liu R, Ning B. Reactive astrogliosis: implications in spinal cord Injury Progression and Therapy. Oxid Med Cell Longev. 2020;2020:9494352.
9. Li Y, Ritzel RM, Khan N, Cao T, He J, Lei Z, et al. Delayed microglial depletion after spinal cord injury reduces chronic inflammation and neurodegeneration in the brain and improves neurological recovery in male mice. Theranostics. 2020;10(25):11376–403.
10. Zhang H, Younsi A, Zheng G, Tail M, Harms AK, Roth J, et al. Sonic hedgehog modulates the inflammatory response and improves functional recovery after spinal cord injury in a thoracic contusion-compression model. Eur Spine J. 2021;30(6):1509–20.
11. Basso DM, Beattie MS, Bresnahan JC. A sensitive and reliable locomotor rating scale for open field testing in rats. J Neurotrauma. 1995;12(1):1–21.
12. Kunkel-Bagden E, Dai H-N, Bregman BS. Methods to assess the Development and Recovery of Locomotor Function after spinal cord Injury in rats. Exp Neurol. 1993;119(2):153–64.
13. Younsi A, Zheng G, Riemann L, Scherer M, Zhang H, Tail M et al. Long-Term effects of neural precursor cell transplantation on secondary Injury processes and functional recovery after severe cervical Contusion-Compression spinal cord Injury. Int J Mol Sci. 2021;22(23).
14. Schindelin J, Arganda-Carreras I, Frise E, Kaynig V, Longair M, Pietzsch T, et al. Fiji: an open-source platform for biological-image analysis. Nat Methods. 2012;9(7):676–82.
15. Tail M, Zhang H, Zheng G, Hatami M, Skutella T, Unterberg A et al. The Sonic hedgehog pathway modulates survival, proliferation, and differentiation of neural progenitor cells under inflammatory stress in Vitro. Cells. 2022;11(4).
16. Mo Z, Zeng Z, Liu Y, Zeng L, Fang J, Ma Y. Activation of Wnt/Beta-Catenin signaling pathway as a promising therapeutic candidate for cerebral Ischemia/Reperfusion Injury. Front Pharmacol. 2022;13.
17. Cui Y, Yin Y, Xiao Z, Zhao Y, Chen B, Yang B, et al. LncRNA Neat1 mediates mir-124-induced activation of Wnt/β-catenin signaling in spinal cord neural progenitor cells. Stem Cell Res Ther. 2019;10(1):400.
18. Gao K, Shen Z, Yuan Y, Han D, Song C, Guo Y, et al. Simvastatin inhibits neural cell apoptosis and promotes locomotor recovery via activation of Wnt/β-catenin signaling pathway after spinal cord injury. J Neurochem. 2016;138(1):139–49.
19. Chen S-D, Yang J-L, Hwang W-C, Yang D-I. Emerging roles of Sonic hedgehog in adult neurological diseases: Neurogenesis and Beyond. Int J Mol Sci. 2018;19(8):2423.
20. Ahn S, Joyner AL. In vivo analysis of quiescent adult neural stem cells responding to sonic hedgehog. Nature. 2005;437(7060):894–7.
21. Amankulor NM, Hambardzumyan D, Pyonteck SM, Becher OJ, Joyce JA, Holland EC. Sonic hedgehog pathway activation is induced by acute brain injury and regulated by injury-related inflammation. J Neurosci. 2009;29(33):10299–308.
22. Pitter KL, Tamagno I, Feng X, Ghosal K, Amankulor N, Holland EC, et al. The SHH/Gli pathway is reactivated in reactive glia and drives proliferation in response to neurodegeneration-induced lesions. Glia. 2014;62(10):1595–607.
23. Chang RC-C, Chiu K, Ho Y-S, So K-f. Modulation of neuroimmune responses on Glia in the Central Nervous System: implication in therapeutic intervention against Neuroinflammation. Cell Mol Immunol. 2009;6:317–26.
24. Candelario-Jalil E, Dijkhuizen RM, Magnus T, Neuroinflammation. Stroke, blood-brain barrier dysfunction, and Imaging modalities. Stroke. 2022;53(5):1473–86.
25. Gensel JC, Zhang B. Macrophage activation and its role in repair and pathology after spinal cord injury. Brain Res. 2015;1619:1–11.
26. Gaojian T, Dingfei Q, Linwei L, Xiaowei W, Zheng Z, Wei L, et al. Parthenolide promotes the repair of spinal cord injury by modulating M1/M2 polarization via the NF-κB and STAT 1/3 signaling pathway. Cell Death Discov. 2020;6(1):97.
27. Fan H, Tang HB, Shan LQ, Liu SC, Huang DG, Chen X, et al. Quercetin prevents necroptosis of oligodendrocytes by inhibiting macrophages/microglia polarization to M1 phenotype after spinal cord injury in rats. J Neuroinflammation. 2019;16(1):206.
28. Chen W, Zhang Y, Yang S, Sun J, Qiu H, Hu X, et al. NeuroRegen Scaffolds combined with autologous bone marrow mononuclear cells for the repair of Acute Complete spinal cord Injury: a 3-Year clinical study. Cell Transpl. 2020;29:963689720950637.
29. Hogaboom N, Malanga G, Cherian C, Dyson-Hudson T. A pilot study to evaluate micro-fragmented adipose tissue injection under ultrasound guidance for the treatment of refractory rotator cuff disease in wheelchair users with spinal cord injury. J Spinal Cord Med. 2021;44(6):886–95.
30. Sari IN, Phi LTH, Jun N, Wijaya YT, Lee S, Kwon HY. Hedgehog signaling in Cancer: a prospective therapeutic target for eradicating Cancer Stem cells. Cells. 2018;7(11).
31. Skoda AM, Simovic D, Karin V, Kardum V, Vranic S, Serman L. The role of the hedgehog signaling pathway in cancer: a comprehensive review. Bosn J Basic Med Sci. 2018;18(1):8–20.
32. Riobo-Del Galdo NA, Lara Montero A, Wertheimer EV. Role of hedgehog signaling in breast Cancer: Pathogenesis and therapeutics. Cells. 2019;8(4).
33. Chen SD, Yang JL, Hwang WC, Yang DI. Emerging roles of Sonic hedgehog in adult neurological diseases: Neurogenesis and Beyond. Int J Mol Sci. 2018;19(8).
34. Ewan EE, Hagg T. Intrathecal Acetyl-L-Carnitine protects tissue and improves function after a mild Contusive spinal cord Injury in rats. J Neurotrauma. 2016;33(3):269–77.
35. Suzuki H, Ahuja CS, Salewski RP, Li L, Satkunendrarajah K, Nagoshi N, et al. Neural stem cell mediated recovery is enhanced by Chondroitinase ABC pretreatment in chronic cervical spinal cord injury. PLoS ONE. 2017;12(8):e0182339.
36. O'Carroll SJ, Gorrie CA, Velamoor S, Green CR, Nicholson LF. Connexin43 mimetic peptide is neuroprotective and improves function following spinal cord injury. Neurosci Res. 2013;75(3):256–67.
37. Characterization of Vascular. Disruption and blood–spinal cord barrier permeability following traumatic spinal cord Injury. J Neurotrauma. 2014;31(6):541–52.
38. Jin LY, Li J, Wang KF, Xia WW, Zhu ZQ, Wang CR, et al. Blood-spinal cord barrier in spinal cord Injury: a review. J Neurotrauma. 2021;38(9):1203–24.
39. Alvarez JI, Dodelet-Devillers A, Kebir H, Ifergan I, Fabre PJ, Terouz S, et al. The hedgehog pathway promotes blood-brain barrier integrity and CNS immune quiescence. Science. 2011;334(6063):1727–31.
40. Podjaski C, Alvarez JI, Bourbonniere L, Larouche S, Terouz S, Bin JM, et al. Netrin 1 regulates blood-brain barrier function and neuroinflammation. Brain. 2015;138(Pt 6):1598–612.
41. Mani S, Radhakrishnan S, Cheramangalam RN, Harkar S, Rajendran S, Ramanan N. Shh-mediated increase in β-Catenin levels maintains cerebellar Granule Neuron progenitors in Proliferation. Cerebellum. 2020;19(5):645–64.
42. Daneman R, Prat A. The blood–brain barrier. Cold Spring Harb Perspect Biol. 2015;7(1):a020412.
43. Zhao Y, Chen C, Xiao X, Fang L, Cheng X, Chang Y, et al. Teriflunomide promotes blood-brain Barrier Integrity by Upregulating Claudin-1 via the Wnt/β-catenin signaling pathway in multiple sclerosis. Mol Neurobiol. 2024;61(4):1936–52.
44. He W, Lu Q, Sherchan P, Huang L, Hu X, Zhang JH, et al. Activation of Frizzled-7 attenuates blood–brain barrier disruption through Dvl/β-catenin/WISP1 signaling pathway after intracerebral hemorrhage in mice. Fluids Barriers CNS. 2021;18(1):44.
45. Wang Q, Huang X, Su Y, Yin G, Wang S, Yu B, et al. Activation of Wnt/β-catenin pathway mitigates blood–brain barrier dysfunction in Alzheimer's disease. Brain. 2022;145(12):4474–88.
46. Robinson BD, Isbell CL, Anasooya Shaji C, Kurek S Jr., Regner JL, Tharakan B. Quetiapine protects the blood-brain barrier in traumatic brain injury. J Trauma Acute Care Surg. 2018;85(5).
47. Deng L, Lv JQ, Sun L. Experimental treatments to attenuate blood spinal cord barrier rupture in rats with traumatic spinal cord injury: a meta-analysis and systematic review. Front Pharmacol. 2022;13:950368.
48. Huang X, Hussain B, Chang J. Peripheral inflammation and blood-brain barrier disruption: effects and mechanisms. CNS Neurosci Ther. 2021;27(1):36–47.
49. Liebner S, Dijkhuizen RM, Reiss Y, Plate KH, Agalliu D, Constantin G. Functional morphology of the blood-brain barrier in health and disease. Acta Neuropathol. 2018;135(3):311–36.
50. Wang Y, Smith W, Hao D, He B, Kong L. M1 and M2 macrophage polarization and potentially therapeutic naturally occurring compounds. Int Immunopharmacol. 2019;70:459–66.
51. Orecchioni M, Ghosheh Y, Pramod AB, Ley K. Macrophage polarization: different gene signatures in M1(LPS+) vs. classically and M2(LPS-) vs. alternatively activated macrophages. Front Immunol. 2019;10:1084.
52. Yunna C, Mengru H, Lei W, Weidong C. Macrophage M1/M2 polarization. Eur J Pharmacol. 2020;877:173090.
53. Funes SC, Rios M, Escobar-Vera J, Kalergis AM. Implications of macrophage polarization in autoimmunity. Immunology. 2018;154(2):186–95.
54. Hellenbrand DJ, Quinn CM, Piper ZJ, Morehouse CN, Fixel JA, Hanna AS. Inflammation after spinal cord injury: a review of the critical timeline of signaling cues and cellular infiltration. J Neuroinflammation. 2021;18(1):284.

55. Paul S, Chhatar S, Mishra A, Lal G. Natural killer T cell activation increases iNOS(+)CD206(-) M1 macrophage and controls the growth of solid tumor. J Immunother Cancer. 2019;7(1):208.
56. Lee C, Jeong H, Bae Y, Shin K, Kang S, Kim H, et al. Targeting of M2-like tumor-associated macrophages with a melittin-based pro-apoptotic peptide. J Immunother Cancer. 2019;7(1):147.
57. Kao JK, Wang SC, Ho LW, Huang SW, Lee CH, Lee MS, et al. M2-like polarization of THP-1 monocyte-derived macrophages under chronic iron overload. Ann Hematol. 2020;99(3):431–41.
58. Barros Filho TE, Molina AE. Analysis of the sensitivity and reproducibility of the Basso, Beattie, Bresnahan (BBB) scale in Wistar rats. Clin (Sao Paulo). 2008;63(1):103–8.
59. de Barros Filho TEP, Molina AEIS. Analysis of The Sensitivity and Reproducibility Of The Basso, Beattie, Bresnahan (BBB) Scale in Wistar Rats. Clinics (Sao Paulo, Brazil). 2008;63:103–8.
60. Bambakidis NC, Miller RH. Transplantation of oligodendrocyte precursors and sonic hedgehog results in improved function and white matter sparing in the spinal cords of adult rats after contusion. Spine J. 2004;4(1):16–26.
61. Lowry N, Goderie SK, Lederman P, Charniga C, Gooch MR, Gracey KD, et al. The effect of long-term release of shh from implanted biodegradable microspheres on recovery from spinal cord injury in mice. Biomaterials. 2012;33(10):2892–901.
62. Li Z, Wu F, Xu D, Zhi Z, Xu G. Inhibition of TREM1 reduces inflammation and oxidative stress after spinal cord injury (SCI) associated with HO-1 expressions. Biomed Pharmacother. 2019;109:2014–21.
63. Sekiguchi A, Kanno H, Ozawa H, Yamaya S, Itoi E. Rapamycin promotes autophagy and reduces neural tissue damage and locomotor impairment after spinal cord injury in mice. J Neurotrauma. 2012;29(5):946–56.
64. Zheng G, Younsi A, Scherer M, Riemann L, Walter J, Skutella T, et al. The CatWalk XT® gait analysis is closely correlated with tissue damage after cervical spinal cord Injury in rats. Appl Sci. 2021;11(9):4097.

Publisher's note